EUROPEAN ORGANIZATION FOR NUCLEAR RESEARCH
CERN - A & B DIVISION

AB-Note-2004-002-ABP

MEASUREMENTS OF EMITTANCE AND TWISS PARAMETERS IN LINAC 3

COMPARISON BETWEEN MEASUREMENTS AND SIMULATIONS

J. Chamings, V. Coco, A. Lombardi, R. Scrivens

Abstract

In the framework of Linac 3 restudy, emittance, and transmission measurements are taken at all stage of acceleration. The results of these measurements will help to increase the accuracy of beam dynamic simulations. Two methods of calculation of the emittance and Twiss parameters from beam profile measurements are used. Some aspects of the beam dynamic in the LEBT, MEBT and Filter of Linac 3 are highlighted.

Keywords: Linac 3, measurements, emittance, Twiss parameters.

MEASUREMENTS OF EMITTANCE AND TWISS PARAMETERS IN LINAC 3
COMPARISON BETWEEN MEASUREMENTS AND SIMULATIONS

J. Chamings, V. Coco, A. Lombardi, R. Scrivens, 10th January 2004

INTRODUCTION

The purpose of these measurements was to define the values of the horizontal and vertical emittance, Twiss parameters and transmission in the different transfer lines of LINAC 3. The main problem is to measure those parameters without any emittance device in the beam line. The first part treats of the different methods that can be used. The other parts present the results of the measurements on LINAC 3.
The knowledge of these parameters will allow us to have an experimental base for future simulations and to validate those that have already been done.

1 METHODS OF EMITTANCE AND TWISS PARAMETERS CALCULATIONS

1.1 CALCULATION OF EMITTANCE VIA PROFILE MEASUREMENTS

We have used profile measurements to calculate the emittance because we cannot have any emittance measurement device in Linac3. It is theoretically possible to deduce the emittance of a beam from a minimum of three profile measurements. These calculations are based on the relation between the sigma matrix at one point and the size of the beam in three "configurations" downstream. By "configuration", we mean different optics between the evaluation point and the measurements point. That means that we can measure beam profile at three different places downstream or at the same places but with different values for the devices of the line. This method has been implemented in two different ways. The first method, called "σ matrix method", calculates emittance and Twiss parameters by calculating the first coefficient of sigma matrix from measurements (see 1.2). The second method, called "fitting to the measurements", "recreates" by calculation the experimental results and then optimises the input Twiss parameters and emittance, to make the theoretical values (of maximal extend) fit with the experimental ones (see 1.3). Both methods are valid if there is no emittance increase between the calculation point and the measuring point.

1.2 σ MATRIX METHOD

An uncoupled beam can be represented, in one plane of the phase space, by a two by two matrix. This matrix, the sigma matrix, is given, for xx', by:

$$\sigma = \begin{bmatrix} x_m^2 = \sigma_{11} & x_e x_m^{'} = \sigma_{12} \\ x_e^{'} x_m = \sigma_{21} & x_m^{'2} = \sigma_{22} \end{bmatrix} \quad (1.)$$

where x_m and $x_m^{'}$ are the maximum extend in x and $x^{'}$ direction and where x_e and $x_e^{'}$ are the value of $x^{'}$ (respectively x) when $x = x_m$ (respectively $x^{'} = x_m^{'}$). Thus we can obtain σ_{11} by measuring beam size from a profile harp.
Assuming the beam is centred and symmetric, $x_e{}' x_m = x_e x_m{}'$ and then $\sigma_{12} = \sigma_{21}$
Emittance at point I is given by $\varepsilon_i^2 = \det(\sigma_i)$ (2.)

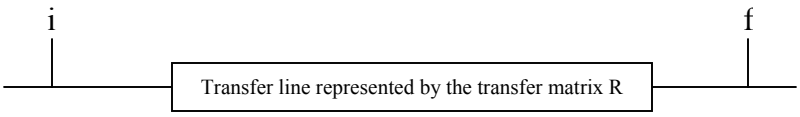

Figure 1.

The evolution of the sigma matrix between i and f (figure 1) is given by (3.1), where *R* in the transfer matrix of the line between i and f:

$$\sigma_f = R\sigma_i R^t \quad (3.1)$$

One can obtain from this equation the relation between the sigma matrix coefficients at point i and f
Writing (3.1) as function of the coefficients of the matrix gives:

$$\begin{aligned}
\sigma_{11f} &= {R_{11}}^2\sigma_{11i} + 2R_{11}R_{12}\sigma_{12i} + {R_{12}}^2\sigma_{22i} \\
\sigma_{12f} &= R_{11}R_{12}\sigma_{11i} + ({R_{12}}^2 + R_{11}R_{22})\sigma_{12i} + R_{12}R_{22}\sigma_{22i} \qquad (3.2) \\
\sigma_{22f} &= {R_{12}}^2\sigma_{11i} + 2R_{22}R_{12}\sigma_{12i} + {R_{22}}^2\sigma_{22i}
\end{aligned}$$

The first equation gives us a relation between the square of the beam size at point f and the sigma matrix at point i. Thus, by measuring n times the beam profile at point f with n known configurations, we obtain the system (4.)

$$\begin{cases}
\sigma_{11f.setting1} = {R_{11.setting1}}^2\sigma_{11i} + 2R_{11.setting1}R_{12.setting1}\sigma_{12i} + {R_{12.setting1}}^2\sigma_{22i} \\
\cdots \\
\sigma_{11f..setting.n} = {R_{11..setting.n}}^2\sigma_{11i} + 2R_{11..setting.n}R_{12..setting.n}\sigma_{12i} + {R_{12.setting.n}}^2\sigma_{22i}
\end{cases} \quad (4.)$$

where σ_{11f} is equal to ${x_m}^2$, see (1.).
By solving this system (which is over determinate if the number of measured configurations is more than 3) one can determine σ_{11i} σ_{12i} and σ_{22i}.
The emittance at point i is given by (1.), one can easily calculate it.

However, several parameters such as the pitch of the profile harp (3.4mm for ITL.MSGHV03) or the approximation in measurements make the accuracy of the method quite low. The reader has to keep in mind that the results are given with ±10%.
We have used a subroutine of TRACE [2], to compute the emittance with σ matrix method. This subroutine is able to determine the ellipse parameters and emittance in the two transverse phase planes from measurements of beam sizes of three or more settings.

1.3 FITTING METHOD

The second way of analysing the measurements was done by fitting the values of measurements.
In effect, the relation (3.1) can be written using the Twiss parameters of the ellipse representing the beam in phase space (5.)

$$\sigma_f = \begin{bmatrix} \beta\varepsilon & -\alpha\varepsilon \\ -\alpha\varepsilon & \gamma\varepsilon \end{bmatrix} \quad (5.)$$

where γ is given by $$\gamma = \frac{1-\alpha^2}{\beta} \quad (6.)$$

By calculating the transfer matrix of the system (7.1),

$$R_{transformation} = R_n . R_{n-1} ..... R_2 . R_1 \qquad (7.1)$$

where R_k is the transfer matrix of the k[th] element of the line.

And writing $$R_{transformation} = \begin{bmatrix} R_{11} & R_{12} \\ R_{21} & R_{22} \end{bmatrix} \quad (5.2)$$

One can write the transformation of the Twiss parameters in matrix notation:

$$\begin{bmatrix} \beta_{f\,(\text{measured})} \\ \alpha_f \\ \gamma_f \end{bmatrix} = \underbrace{\begin{bmatrix} R_{11}^2 & -2R_{11}R_{12} & R_{12}^2 \\ -R_{11}R_{21} & R_{21}R_{12} + R_{11}R_{22} & -R_{12}R_{22} \\ R_{21}^2 & -2R_{21}R_{22} & R_{22}^2 \end{bmatrix}}_{\text{calculated}} \cdot \underbrace{\begin{bmatrix} \beta_i \\ \alpha_i \\ \gamma_i \end{bmatrix}}_{\text{guessed}} \qquad (6.)$$

As the half width x_m of the beam is given by (7.) (see 1. and 5.)

$$x_m = \sqrt{\beta\varepsilon} \qquad (7.)$$

We can determine the theoretical values of x_m in position 1 by knowing the Twiss parameters in position 0. Therefore, we have used an optimisation algorithm of Mathematica [3] (genetic algorithm) in order to find the Twiss Parameters and emittance corresponding to the fit of this "theoretical" scan to the measured one. The advantage over the σ matrix method computed by TRACE is the possibility to control all the parameters of the calculation. More over, it gives the possibility to determine the error of the fitting by using the formula (8.) [4]:

$$\kappa = \frac{1}{N_{measurments}} \sum_{j=1}^{N_{measurments}} \frac{\left(x_{m.theoretical} - x_{m.measurments}\right)^2}{x_{m.theoretical}} \qquad (8.)$$

In order to compare both methods, we have reintroduced the values given by TRACE in the Mathematica calculation to calculate this error. The results of this analysis are shown in 1.4.

2 MEASUREMENTS OF EMITTANCE IN LEBT

2.1 DESCRIPTION OF THE LINE

The LEBT has two goals: to bring the 2.5keV/u lead ion beam from the source to the RFQ and to separate the different charges states that compose it [1].

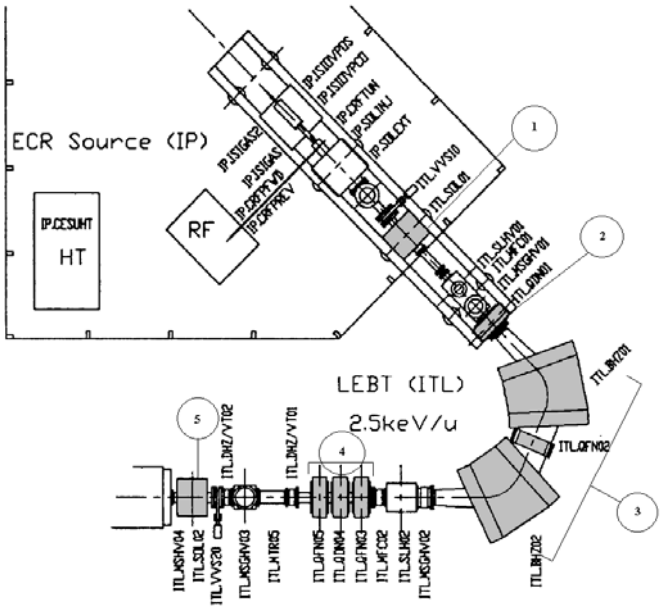

Figure 2: *Schematic layout of LEBT*

The LEBT consists of three main parts (figure 2). A solenoid (ITL.SOL01) between the source and the spectrometer is in charge of bringing a beam as small as possible to the object point of the spectrometer. This is required to avoid any loss of intensity in the spectrometer and to be able to select the charge states. The second part is the spectrometer itself, which is made of a quadrupole (ITL.QDN01) and two bending magnets (ITL.BHZ01, ITL.BHZ02). From the image point of the spectrometer to the entrance of the RFQ, a triplet of quadrupoles (ITL.QFN03, ITL.QDN04, ITL.QFN05) and a solenoid (ITL.SOL02) allow the matching of the beam to the RFQ acceptance.
Three profile harps are placed on this line in order to evaluate the horizontal and vertical profile. The first one (ITL.MSGHV01) is placed after the first solenoid, the second one (ITL.MSGHV02) after the spectrometer and the third one (ITL.MSGHV03) after the triplet.
The nominal beam dynamics in the LEBT is shown in figure 3.

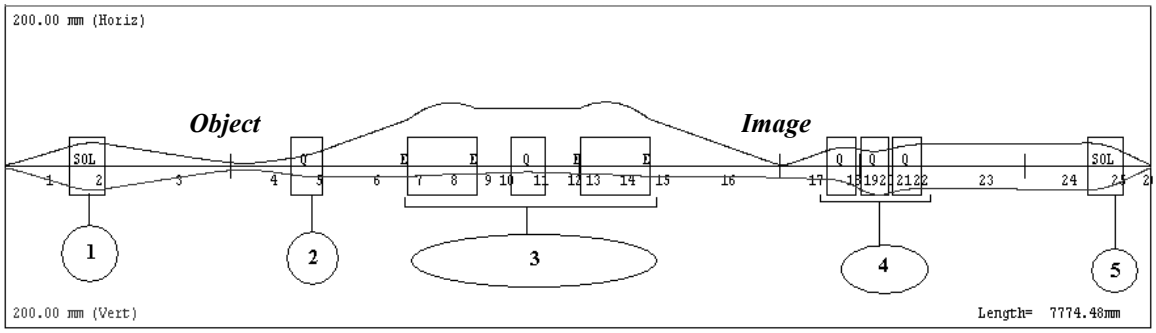

Figure 3: *Horizontal (top) and Vertical (bottom) beam envelopes in LEBT*

2.2 DESCRIPTION OF THE MEASUREMENTS

Emittance measurements were evaluated at two points in the LEBT. The first was immediately after the extraction of the ECR source. The first profile harp had major damage that made it unusable, and so another method to find the beam profile was required. There are spectrometer slits in the same instrument chamber as the harp, and these were stepped across the beam. At each step the intensity of the rest of the beam (which did not hit the slit) was measured further down stream. Differentiating the intensity with respect to the slit position, gave the beam profile at the position of the slits. This method is explained in more detail in [5]. This allowed us to calculate the emittance of the ECR source, by varying the strength of the solenoid ITL.SOL01. Only the fitted method was used here, as TRACE does not allow the transfer matrix to be coupled in the X-Y plane (as is a solenoid), and so could not give any results.
Another set of measurements has been performed in order to evaluate the emittance of the beam after the output of the bending magnets. The measurements have been done with the third profile harp of the line (ITL.MSG03). The reason why we have chosen the third profile harp is that between this point and spectrometer output, the line is only constituted by quadrupoles and drifts, avoiding any emittance increase. The other good point of this configuration is to be able to reduce the sigma matrix and transfer matrix to a two by two matrix. In effect, there is no coupling between horizontal and vertical components in quadrupoles and drifts.
The first set of measurements has been performed with the reference optics of the LEBT. The three quadrupoles of the triplet have been scanned. By "scanned", one should understand that we have changed several times the values of the elements in order to change the optic of the line (see 1.1).
The second set of measurements has been performed with values of the fields in the bending magnets corresponding to the values to set the Pb27+ on the reference trajectories. The settings of the triplet were more or less the same as in the first set. Only the third quadrupole has been scanned.
The third set of measurements has been performed in relation to the simulations. Pb27+ is on the reference trajectory; the first solenoid was supposed to be set in a way to avoid any collision with the vacuum chamber and to keep the waist of the beam on the image point of the spectrometer. Only the third quadrupole has been scanned. But we have realised later that the waist was not found for these settings and that we were maybe losing beam in the first solenoid [5]. Therefore, the only interest of these settings becomes the comparison between manual optimization and simulation optimization (see 3.1).
One can see, in table 4, the exact settings that were used.

	First Set			Second Set			Third Set		
Device	**Current (A)**	**Field**		**Current (A)**	**Field**		**Current (A)**	**Field**	
ITL.SOL01	130.39	0.3794	T	131.95	0.384	T	122.11	0.3553	T
ITL.QDN01	-10.99	-0.312116	T/m	-11.06	-0.314104	T/m	-25.03	-0.710852	T/m
ITL.BHZ01	80.96	0.14110399	T	81.31	0.141714	T	81.31	0.141714	T
ITL.BHZ02	81.42	0.141905717	T	81.31	0.141714	T	81.31	0.141714	T
ITL.QFN03	32.99	0.9224004	T/m	48.33	1.3513	T/m	48.35	1.351866	T/m
ITL.QDN04	-50.99	-1.443017	T/m	-58.41	-1.653	T/m	-63.61	-1.800163	T/m
ITL.QFN05	27.01	0.764383	T/m	Variable	Variable		Variable	Variable	

Table 4: *Settings used in LEBT measurements*

2.3 RESULTS OF THE MEASUREMENTS

We have done each set of measurements around a waist of the beam. In effect, it gives a better description of the function followed by the maximal extension, and reduces the space of solutions, reducing the error of the method.
Without any calculations, the fact we are able to observe the waists at the expected place already gives us indications upon the validity of the description of beam dynamic in our simulations.
Figure 5.0.1 shows the result of the solenoid (ITL.SOL01) scan (see also [5]), this gives the horizontal and vertical beam widths as a function of the solenoid strength, and also shows the fitted curve placed on the

measured points. It can be seen, that the horizontal and vertical beam widths are similar, this means that we have a symmetrical beam at this point, and so the beam parameters will be similar for both planes. The measured beam parameters found are shown in Table 5.0.2

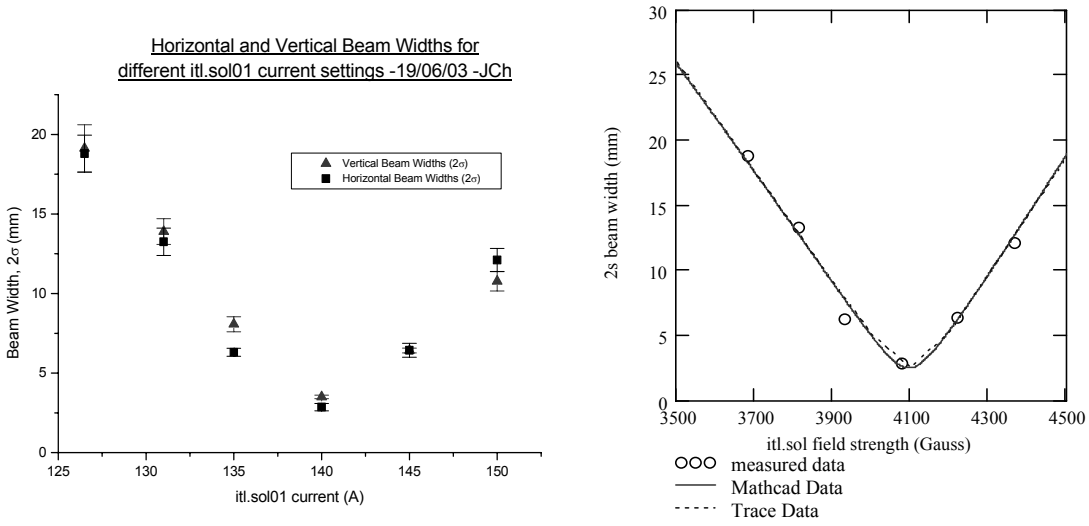

Figure 5.0.1: *Horizontal and Vertical Beam widths at the spectrometer slits (object point) as a function of ITL.SOL01 strength, with the fitted curve (right)*

$\alpha_{x\ \&\ y}$	$\beta_{x\ \&\ y}$	ε_{4rms} (mm.mrad)
-0.89	0.04	100

Table 5.0.2: *The results of the horizontal and vertical beam parameters after the ECR source in the LEBT.*

In the following are presented: the results of measurements (cross marked), the σ matrix method calculation (square marked), and the fitting method calculation (triangle marked), for the scans of the quadrupole triplet.
For the first setting, the figures 5.1.1.h and 5.1.1.v represent the horizontal and vertical scan of ITL.QFN03, the figures 5.1.2.h and 5.1.2.v represent the horizontal and vertical scan of ITL.QDN04, the figures 5.1.3.h and 5.1.3.v represent the horizontal and vertical scan of ITL.QFN05.
For the second setting, the figures 5.2.h and 5.2.v represent the horizontal and vertical scan of ITL.QFN03
For the third setting, the figures 5.3.h and 5.3.v represent the horizontal and vertical scan of ITL.QFN03

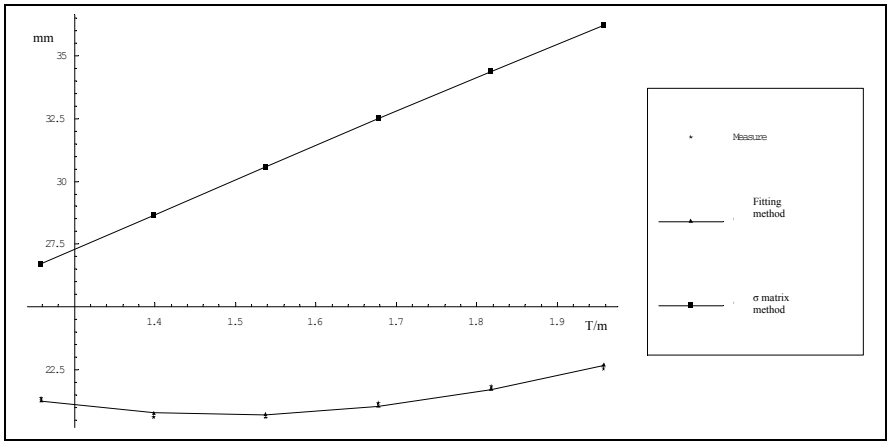

Figure 5.1.1.h: *Horizontal beam size (mm) at ITL.MSG03 vs. ITL.QFN03 gradient (T/m) for the first setting*

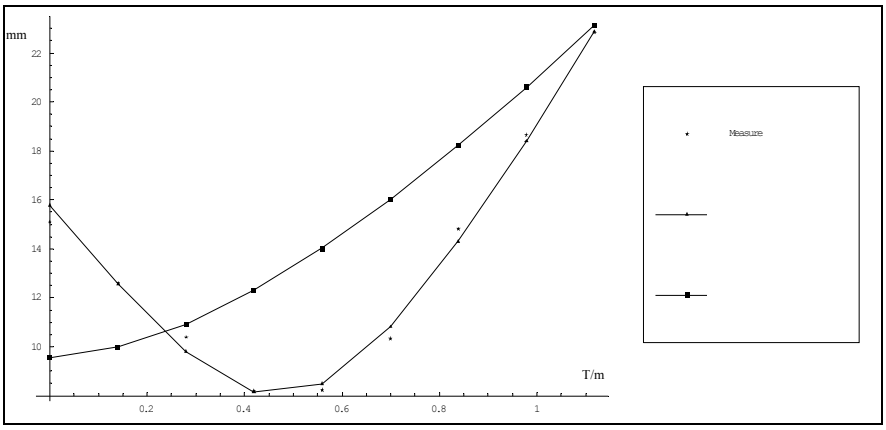

Figure 5.1.1.v: *Vertical beam size (mm) at ITL.MSG03 vs. ITL.QFN03 gradient (T/m) for the first setting*

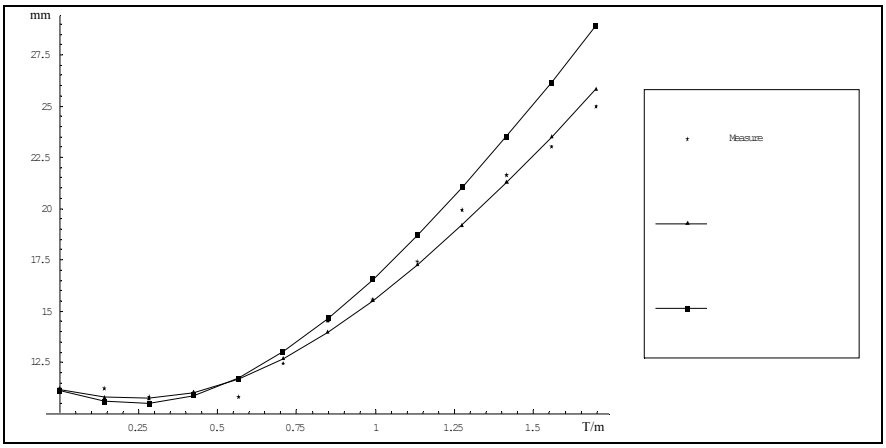

Figure 5.1.2.h: *Horizontal beam size (mm) at ITL.MSG03 vs. ITL.QDN04 gradient (T/m) for the first setting*

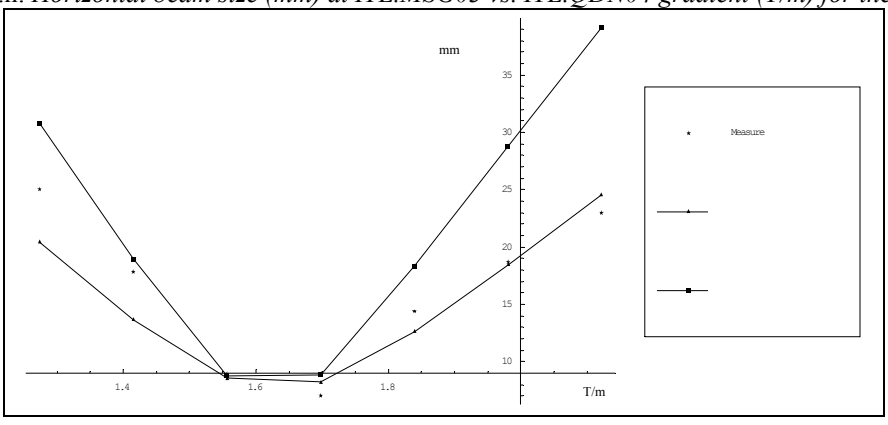

Figure 5.1.1.v: *Vertical beam size (mm) at ITL.MSG03 vs. ITL.QDN04 gradient (T/m) for the first setting*

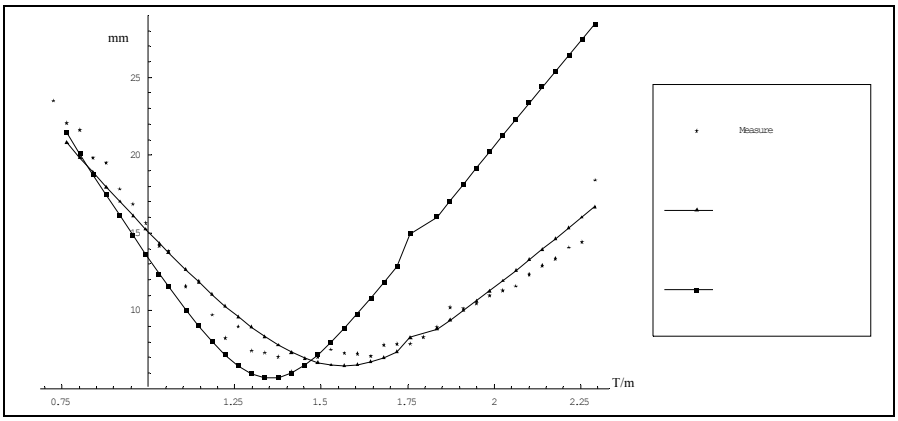

Figure 5.1.3.h: *Horizontal beam size (mm) at ITL.MSG03 vs. ITL.QFN05 gradient (T/m) for the first setting*

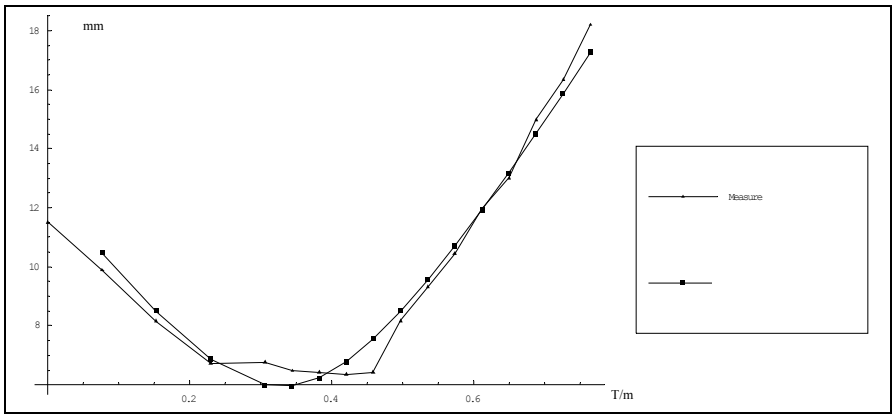

Figure 5.1.3.v: *Vertical beam size (mm) at ITL.MSG03 vs. ITL.QFN05 gradient (T/m) for the first setting*

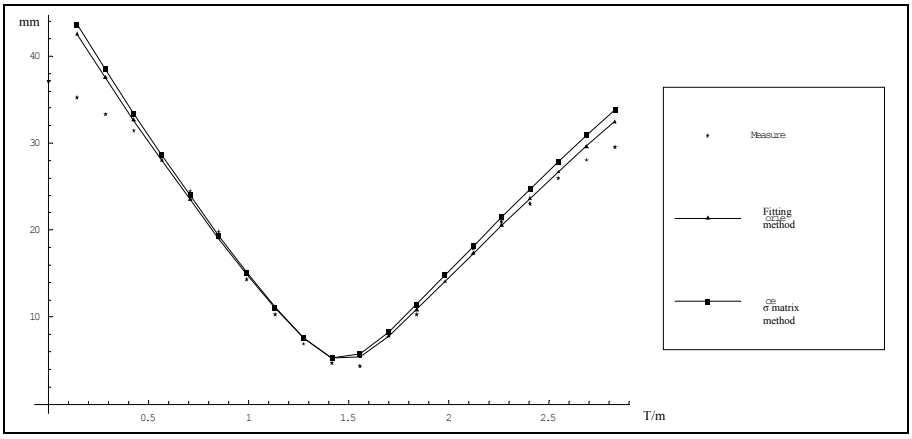

Figure 5.2.h: *Horizontal beam size (mm) at ITL.MSG03 vs. ITL.QFN05 gradient (T/m) for the second setting*

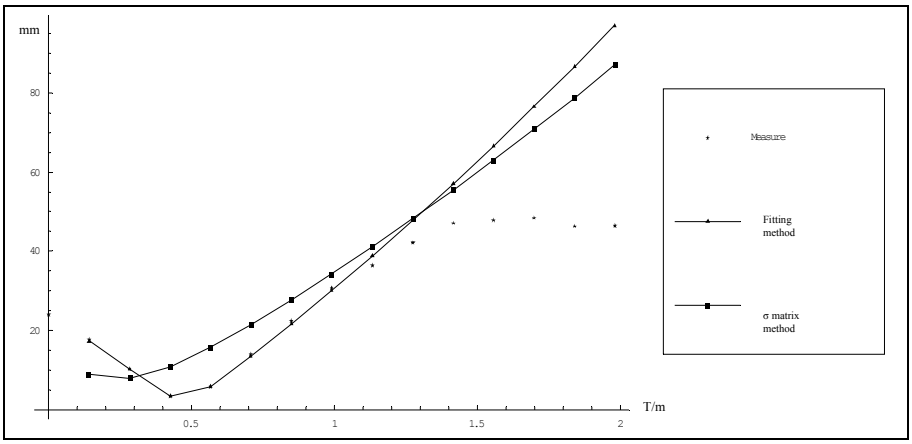

Figure 5.2.v: *Vertical beam size (mm) at ITL.MSG03 vs. ITL.QFN05 gradient (T/m) for the second setting*

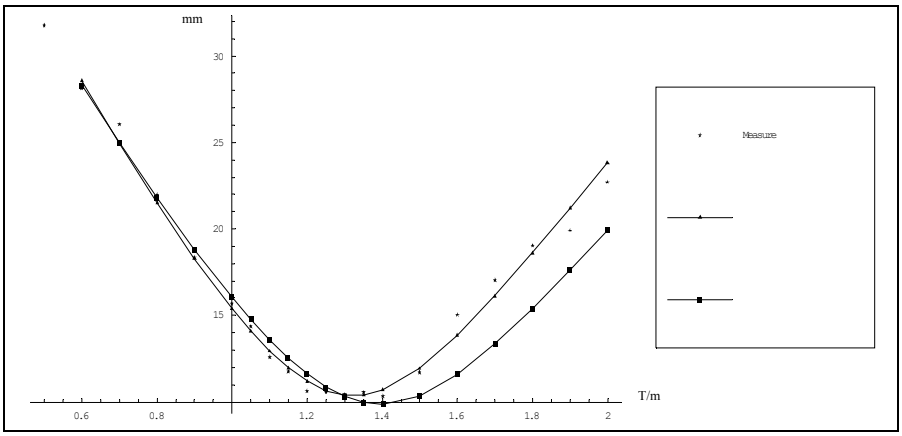

Figure 5.3.h: *Horizontal beam size (mm) at ITL.MSG03 vs. ITL.QFN05 gradient (T/m) for the third setting*

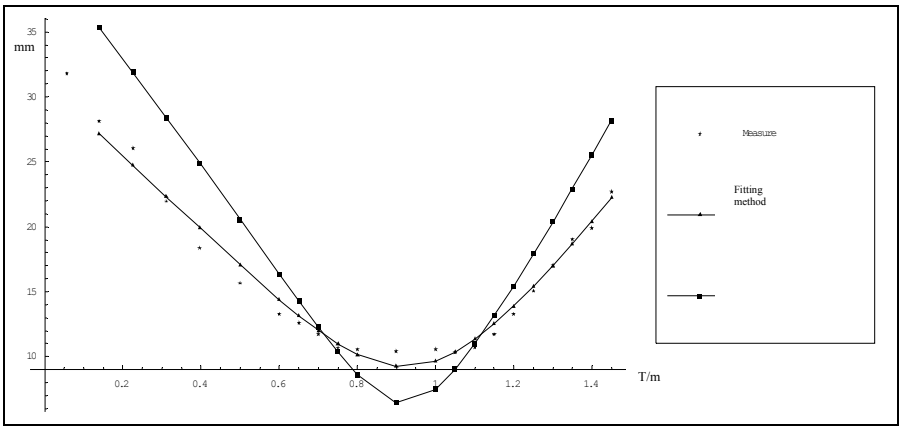

Figure 5.3.v: *Vertical beam size (mm) at ITL.MSG03 vs. ITL.QFN05 gradient (T/m) for the third setting*

In the following table (Table 6), the Twiss parameters (ax, ay, bx, by), emittance (Ex, Ey), and error (ksi) for both planes at the second bending magnet output are presented. The average is weighted with ksi. Emittances are in mm.mrad, beta is in mm/mrad, and alpha has no dimension.

			horizontal				vertical			
			Ex mm.mrad	ax	bx mm/mrad	ksi	Ey mm.mrad	ay	by mm/mrad	ksi
First set	ITL.QFN03	Trace	93.8596	4.596	7.0588	3.38504	66.8256	11.312	12.6811	1.16741
		Mathematica	134.936	4.8743	5.60188	0.000768	94.8544	5.66901	5.48225	0.013132
	ITL.QDN04	Trace	133.28	4.854	5.5938	0.109422	94.7068	5.67	5.4929	1.78804
		Mathematica	118.826	4.32371	5.1353	0.014577	74.3367	5.95856	6.39598	0.133984
	ITL.QFN05	Trace	113.176	4.393	5.2837	1.8062				
		Mathematica	93.5571	4.02567	6.18649	0.081226	87.2029	6.65826	6.9916	0.029519
	Average	Trace	130.99966	4.820815	5.6199414	0.300361	77.8387424	9.083396	9.841743367	1.41256
		Mathematica	133.768317	4.839428	5.58393681	0.00217	91.344768	5.972644	5.975500581	0.025534
Second set	ITL.QFN05	Trace	91.3668	4.951	6.0963	0.062266	135.5056	14.537	17.2825	3.17402
		Mathematica	85.6601	4.87876	6.07736	0.051935	53.325	21.2391	21.5115	0.028165
Third set	ITL.QFN05	Trace	185.1414	2.809	3.0898	0.207244	112.8246	3.504	3.83045	0.802171
		Mathematica	213.183	3.18803	3.24171	0.021789	119.987	3.01098	3.36827	0.048346

Table 6: *Emittance and Twiss parameters at spectrometer output for the three settings.*

2.4 ANALYSIS OF THE RESULTS

First of all, the results given by the both methods seam to be quite close and the error for each calculation allows a good confidence in the results.
Previous measurements [1] give the emittance around 120mm.mrad of the source, and the results of the first solenoid scan agree with this. From recent simulations (RS Note 2003-20), it has been suggested that the beam is hitting the vacuum chamber walls at, or before the solenoid. TRACE was used to investigate this with the new measured beam parameters. This is shown in figure 7.1, and it can be seen that the beam does appear to be limited by the chamber walls. Further investigation of this is due to be carried out.

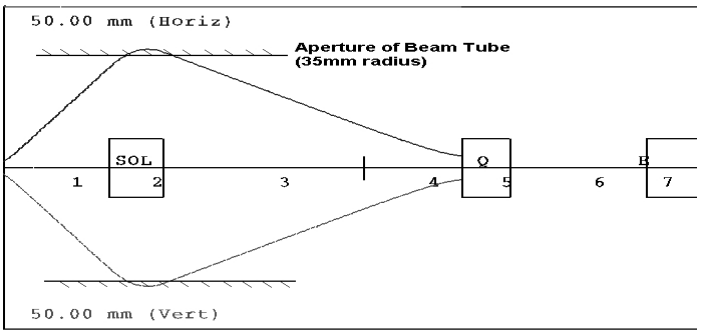

Figure 7.1: *Trace beam showing the physical aperture of the beam tube*

Running the measured values of source parameters with Path manager, we obtain for first setting, at spectrometer output: $\alpha x = 5.3$, $\beta x = 6$mm/mrad, $\alpha y = 1.9$ and $\beta y = 0.64$mm/mrad. Compared to the results in table 6, the horizontal values, with respect to the method accuracy are very close for horizontal parameters but quite different for vertical one. In fact if we run the simulation until the second quadrupole of the triplet, one can note that the beam hits vertically the vacuum chamber. Therefore, the values of vertical emittance correspond to a beam, which would have a maximal extend of 56mm (radius of the vacuum chamber) at the second quadrupole. For this reason, we cannot trust the values of emittance in vertical plane. Another interesting point is that if we run the simulation of what should be the real beam until the RFQ input, with the values of the quadrupoles and solenoid of §3.2, we can see that the beam is more or less matched but has an emittance increase due to the fact the beam does not enter symmetrically in the solenoid. This seams to explain that, in §4.3 we found a higher emittance than expected at the RFQ output. All details of these simulations are given in the appendix.
For the triplet measurements, if we consider the first setting as the nominal one, one can distinguish the results of the second and of the third settings. In effect, we have a lower emittance in second setting and a higher emittance in third one.

The lower emittance in second setting comes from the fact that beam hits the vacuum chamber, in vertical plane (see second setting in figure 8). For the higher emittance in third setting, we suppose that it's due to the fact the sextupole component seen by the beam in the bending magnets, stops being negligible when the beam enters the spectrometer with a large and defocused beam in vertical plane. This is shown in figure 7.2 that represents the simulation with TRACE of the envelope of the beam in the first part of LEBT for the third setting.

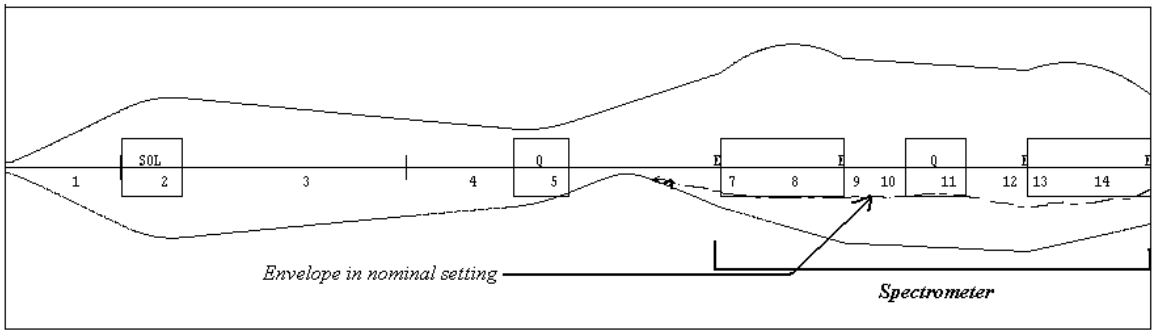

Figure 7.2: *Beam envelope in third setting compared to nominal one*

3 OPTIMIZATION OF THE SETTINGS IN LEBT

3.1 DESCRIPTION OF THE MEASUREMENTS

The second part of the comparison between simulations and measurements was realised in the following way.
Once the Twiss parameters of these three settings had been calculated, we have introduced those parameters in the simulations in order to find the settings, in the triplet and solenoid after the spectrometer, that give the correct matching to RFQ. The beam dynamics of these configurations, with measured values as input, is given in figure 8 and the settings are summarised in figure 9.

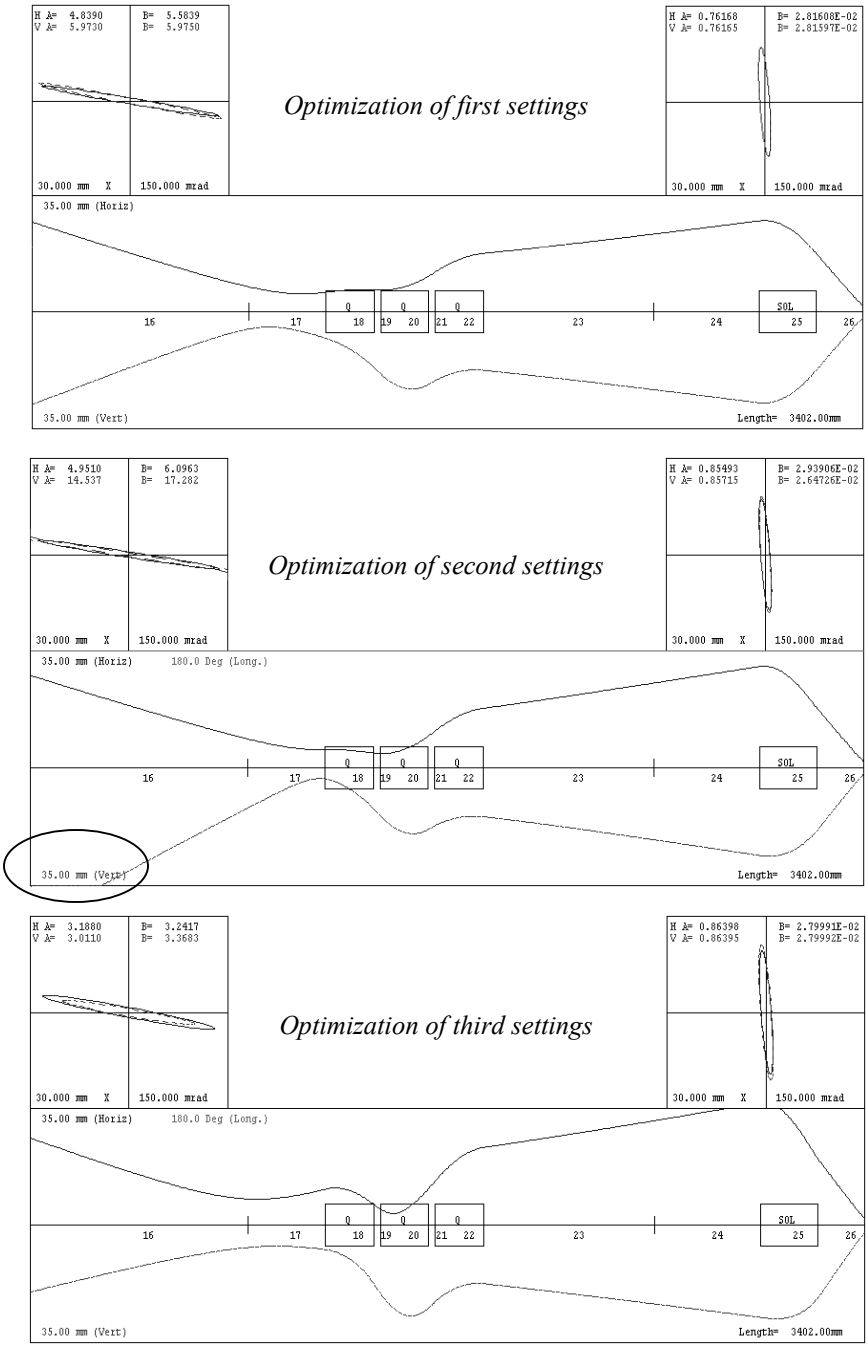

Figure 8: *Beam Dynamic of the expected optimised settings from the spectrometer output*

Using the settings of the first part, we have changed step by step the values of the elements of the triplet and of the second solenoid in order to increase the intensity in the faraday cup placed just after the RFQ. In effect, the more intensity we have at the exit of RFQ, the more we can assume to be close to the matching parameters at the entrance of RFQ.

3.2 RESULTS AND ANALYSIS OF THE MEASUREMENTS

The results of these measurements are summarized in table 9.

Optimisation of the settings throught RFQ	Standard	First Settings		Second Settings		Third Settings	
		Calculated	Empirically Optimised	Calculated	Emirically Optimised	Calculated	Empirically Optimised
ITL.QFN03 (A)	33	38.71	40	65.6	60.5	87.82	78
ITL.QDN04 (A)	51	-54.2	-55.25	-64.7	-63.5	-69.12	-75.5
ITL.QFN05 (A)	27	27.5	29	30.58	31	39.03	33
ITL.SOL02 (A)	159.5	158	158.5	157.55	161.5	158.32	175.5
Intensity (microamps)	79	77	80	69	72	26	40

Table 9: *Settings of solenoids and quadrupoles used for optimisation*

The first thing we can note is that in the two first settings, the results of the scans are very close to what was expected from simulation. For the triplet, the difference between simulation and measurements doesn't exceed 10% (5% for the first setting). This value is within the accuracy of the method.
For the solenoid (ITL.SOL02) the difference is higher but we can expect an error in calibration. We have between Intensity in the solenoid and field in it, the following relation:

$$Field = Current.in.coils * CalibrationFactor$$

Assuming the calculated value in gauss of solenoid field in the first set is corresponding to the optimised value of intensity in A, we can establish a new calibration factor of 29.1 gauss/A instead of 33.2 gauss/A used until now, which gives better results (less than 10% of difference even in the third set). It also corresponds to the calibration factor of solenoid one (ITL.SOL01) found in [5].
Because of these results, we can conclude that once we know the input Twiss parameters, we are able to simulate the dynamic of the beam in quadrupoles and solenoids.

4 MEASUREMENTS OF EMITTANCE IN MEBT

4.1 DESCRIPTION OF THE LINE

The goal of the MEBT is to bring the 250keV/u lead ion beam from the RFQ to the IH [1].

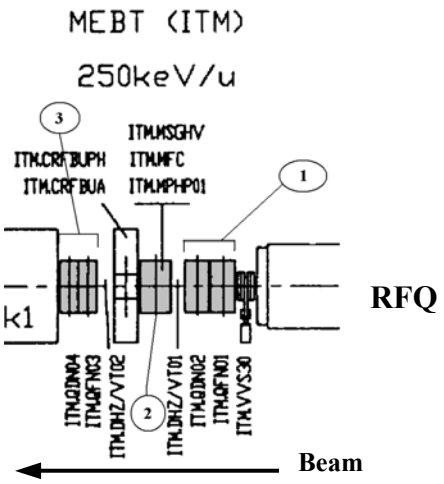

Figure 10: *Schematic layout of MEBT*

The MEBT consists of three main parts (figure 10). The first and the third one, composed of two times two quadrupoles (respectively ITM.QFN01, ITM.QDN02 and ITM.QFN03, ITM.QDN04) are in charge to match the beam to the transverse acceptance of the IH. In effect, we have four parameters to match and four degrees of liberty (the gradient of the four quadrupoles). The second part, composed of buncher and drift, is in charge to match the two longitudinal parameters to longitudinal IH acceptance. The first two quadrupoles are also in charge of bringing a small round beam to the buncher in order to avoid any increase of transverse emittance in it.
A profile harp (ITM.MSGHV) is placed just after the first doublet, in order to evaluate the horizontal and vertical profile of the beam. One can see in figure 11 the nominal beam dynamics in the MEBT.

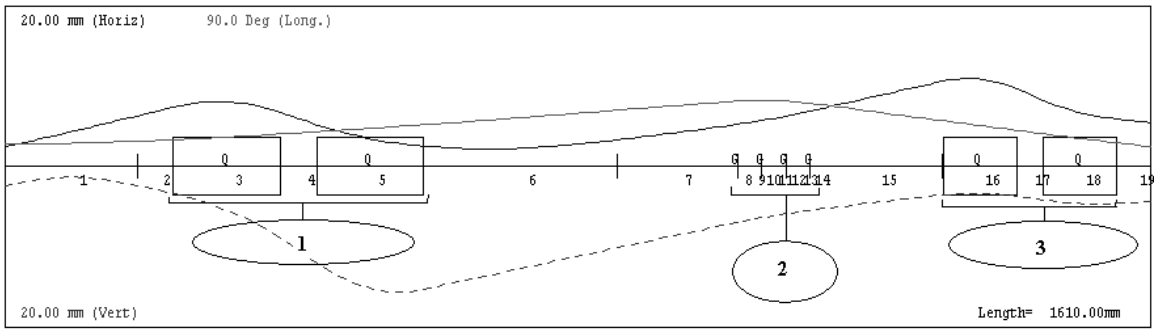

Figure 11: *Horizontal (top) and Vertical (bottom) beam envelopes in MEBT*

4.2 DESCRIPTION OF THE MEASUREMENTS

One can see, on table 12, the settings that were used in MEBT.

Device	Current (A)	Field (T)
ITL.QFN01	99.692	22.63
ITL.QDN02	variable	variable

Table 12: *Settings used in MEBT measurements*

To determine the Twiss parameters at the exit of RFQ, we have measured the beam profile on the profile harp ITM.MSG04 for different values of ITM.QDN02.
The same methods of calculation than in LEBT have been used to determine emittance, alpha and beta (see 1.3).

4.3 RESULTS OF THE MEASUREMENTS

The results of these measurements are shown in figure 13. We have only done the measurements in horizontal plane because we were not able to have a waist in the vertical plane. The quadrupole field limits didn't allow us to find this position.

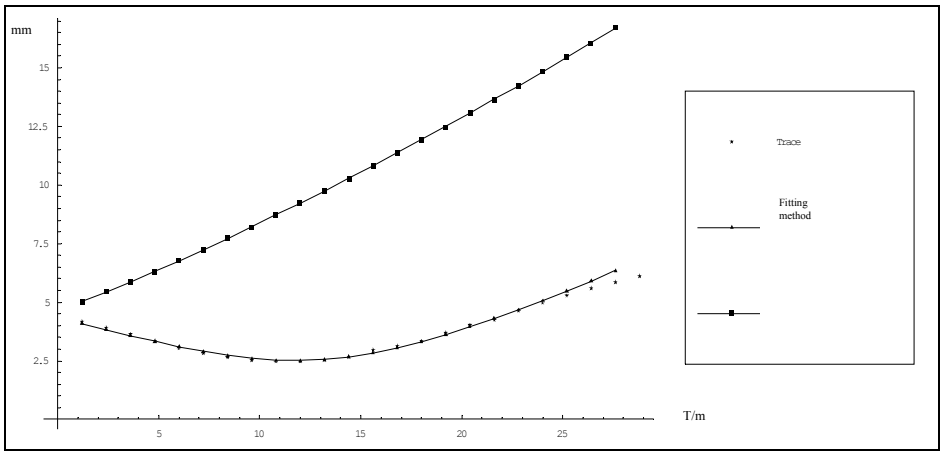

Figure 13: *Horizontal beam size (mm) at ITM.MSHV vs. ITM.QDN02 gradient (T/m) for nominal setting*

As the losses in RFQ are very small we can calculate the expected value of emittance in MEBT by using the conservation of normalized emittance (5.).

$$\varepsilon_N = \varepsilon\beta\gamma \qquad (5.)$$

where ε is the physical emittance and β, γ the relativistic parameters.
We know that normalized emittance (6.) is conserved during acceleration.

$$\varepsilon_{N_{LEBT}} = \varepsilon_{N_{MEBT}} \quad (6.)$$

Therefore, we can link LEBT and MEBT emittance in relation (7).

$$\varepsilon_{MEBT} = \frac{\beta_{LEBT}\gamma_{LEBT}}{\beta_{MEBT}\gamma_{MEBT}}.\varepsilon_{LEBT} \qquad (7.)$$

Or, by writing β in function of γ :

$$\gamma = \frac{1}{\sqrt{1-\beta^2}} \quad (8.)$$

$$\varepsilon_{MEBT} = \sqrt{\frac{\gamma_{LEBT}^{\ 2}-1}{\gamma_{MEBT}^{\ 2}-1}}.\varepsilon_{LEBT} \qquad (9.)$$

Equation (9.) for the nominal setting (setting 1 of §2.3) of LEBT (emittance around 120mm.mrad) gives the following result:

$$\varepsilon_{MEBT} = 12 mm.mrad$$

The results of the measurements give an emittance around 20mm.mrad. Hence we can suppose we have an increase of emittance in RFQ, which can be due to a small mismatch of the beam at the entrance and to the fact we use Pb27+ instead of Pb25+.

Twiss parameters (αx, βx), emittance (Ex), and error (ksi) for both planes at RFQ output are presented in table 14. Emittances are in mm.mrad, beta is in mm/mrad, and alpha has no dimension.

		horizontal			
		Ex	ax	bx	ksi
ITM.QDN02	Trace	29.7032	1.891	0.2858	4.3677
	Mathematica	21.6579	-1.15825	0.178848	0.001828
Expected from PARMTEQ		13.5	- 1.4	0.2	

Table 14: *Twiss parameters and emittance at RFQ output*

The reader can notice that the results for αx are of opposite sign between Trace and Mathematica. For the final choice, we will prefer the negative result. First because the ksi of fitting method is much lower than the one of σ matrix. Then, physically, the beam is supposed to be divergent at our RFQ output.

5 MEASUREMENTS OF EMITTANCE IN THE FILTER LINE

5.1 DESCRIPTION OF THE LINE

The goal of the FILTER is to bring the 4.2MeV/u lead ion beam from the IH Linac to the PSB injection, running through a stripping foil, giving Pb53+ [1].
The FILTER consists of four main parts (figure 15). A triplet of quadrupoles (ITF.QFN01S, ITF.QDN02, ITF.QFN03S) between the IH Linac and the stripping foil is in charge of bringing a focused beam as small as possible to the stripper in order to avoid any emittance increase due to scattering of the beam. The second part is the stripping foil (ITL.STR01), which gives a Pb53+, Pb52+ and Pb54+ beam from the Pb27+. From the stripping foil to the filter, a second triplet of quadrupoles (ITF.QFN04, ITF.QDN05, ITF.QFN06) is in charge of matching the beam to the filter section. The last part, the filtering section, is made of four bending magnets (ITF.BHZ11, ITF.BHZ12, ITF.BHZ13, ITF.BHZ14). The first two correspond to a translating system and therefore allow the separation of the different charges states, while the final two align the trajectory of the reference particle and prepare the beam for a non-dispersive transfer.

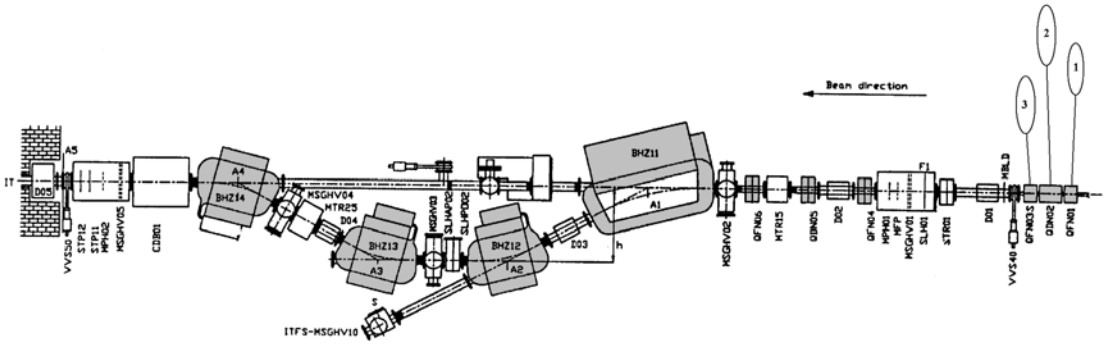

Figure 15: *Schematic layout of Filter*

Four profile harps (ITF.MSGHV02, ITF.MSGHV03, ITF.MSGHV04, ITF.MSGHV05) are placed along the line, in order to evaluate the horizontal and vertical profile of the beam and to analyze the composition of the beam. For the measurements of emittance, we have used ITF.MSGHV02, which is placed right after the second triplet. One can see in figure 16 the nominal beam dynamic of the filter from triplet to profile harp.

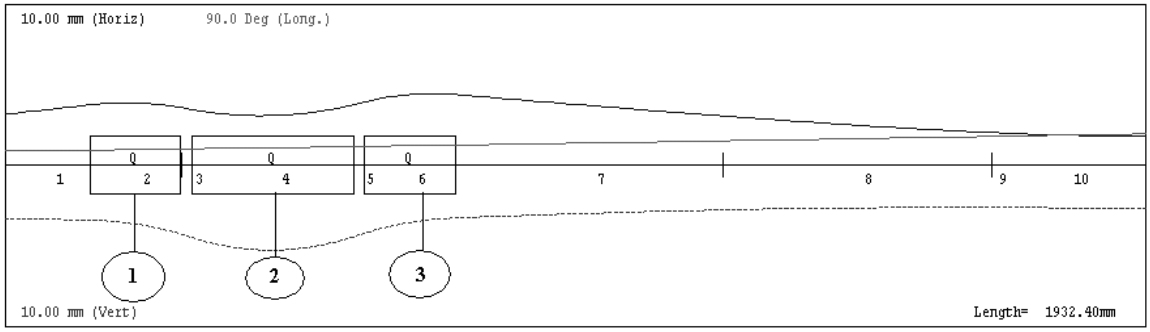

Figure 16: *Horizontal (top) and Vertical (bottom) beam envelopes in Filter*

5.2 DESCRIPTION OF THE MEASUREMENTS

One can see, in table 17, the settings that were used in FILTER.

Device	Current (A)	Field (T)
ITF.QFN01S	119.5	35.250
ITF.QDN02	-129.09	-38.079
ITF.QFN03S	119.5	35.250

Table 17: *Settings used in Filter measurements*

To determine the Twiss parameters at the exit of IH Linac, we have scanned both first and second quadrupoles of the first triplet (ITF.QFN03S, ITF.QDN02) in order to measure the profile of the beam in profile harp before the bending magnet.
The same method of calculation as in LEBT has been used to determine emittance, alpha and beta (see 1.3).

5.3 RESULTS OF THE MEASUREMENTS

All the results of these measurements are shown in the following figures. Figure 18.1.h and 18.1.v represent the horizontal and vertical scans of ITF.QFN01S. Figure 18.2.h and 18.2.v represent the horizontal and vertical scan of ITF.QDN02.

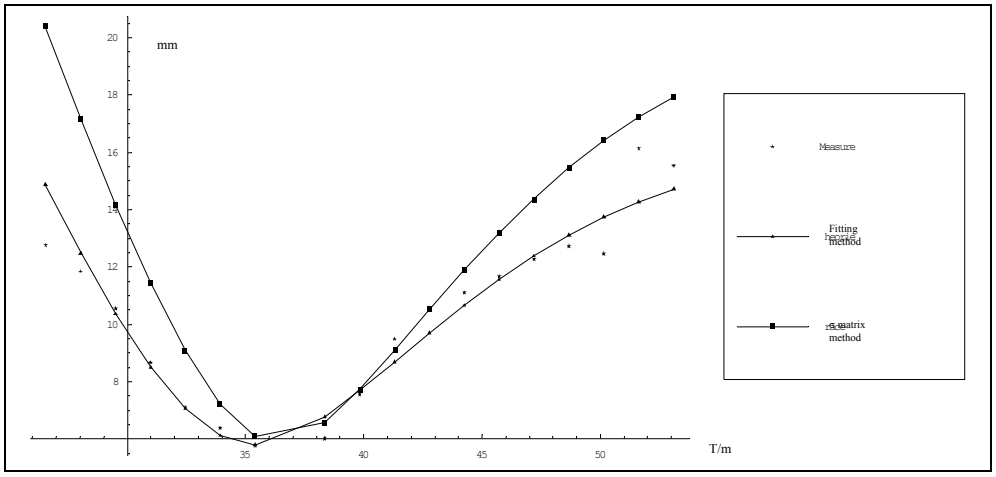

Figure 18.1.h: *Horizontal beam size (mm) at ITF.MSG02 vs. ITF.QFN03S gradient (T/m) for nominal setting*

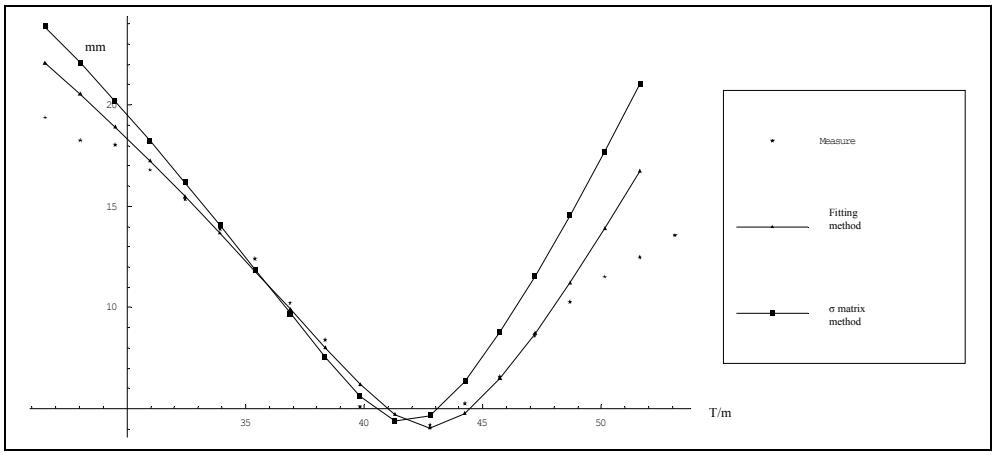

Figure 18.1.v: *Vertical beam size (mm) at ITF.MSG02 vs. ITF.QFN03S gradient (T/m) for nominal setting*

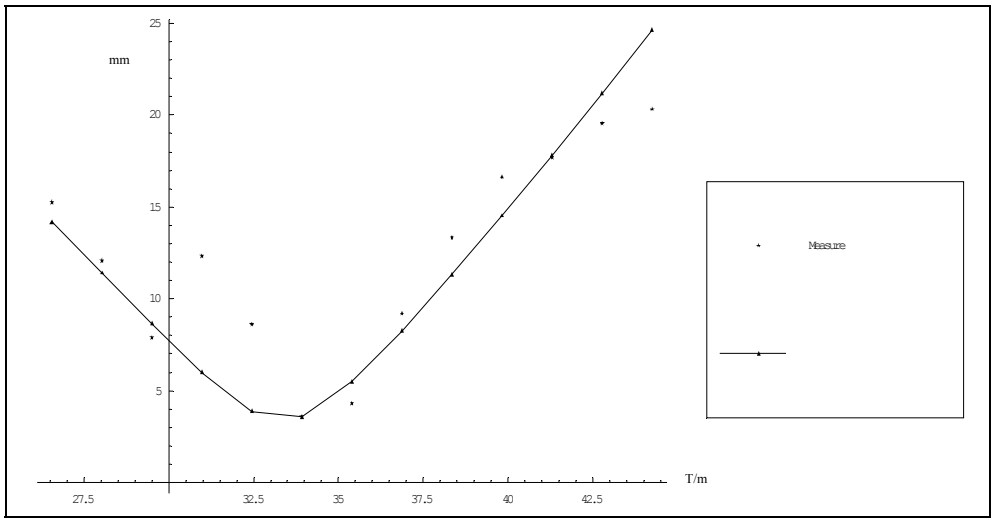

Figure 18.2.h: *Horizontal beam size (mm) at ITF.MSG02 vs. ITF.QDN02 gradient (T/m) for nominal setting*

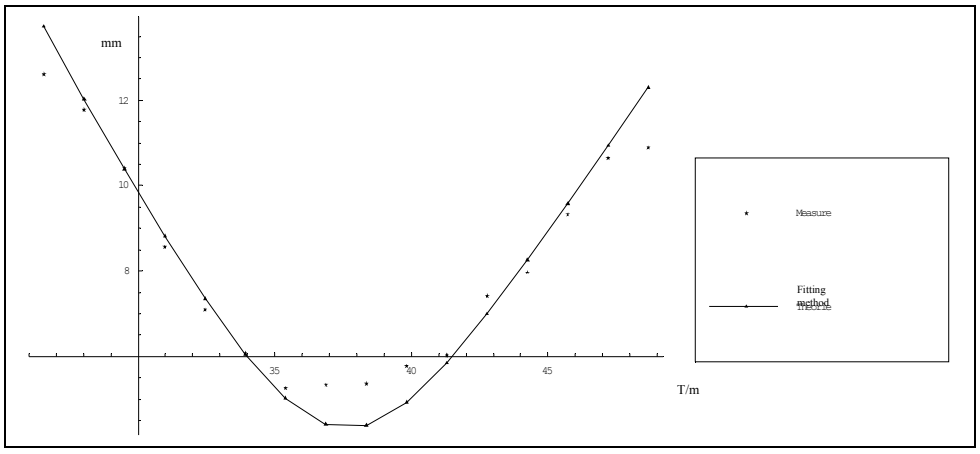

Figure 18.2.v: *Vertical beam size (mm) at ITF.MSG02 vs. ITF.QDN02 gradient (T/m) for nominal setting*

By using the same calculation than for MEBT, equation (8.) gives, with the measured values of MEBT (ε=20mm.mrad) emittance, the following result:

$$\varepsilon_{FILTER} = 9.5mm.mrad$$

The scan of ITF.QFN03S gives quite good results. Emittance is around 7mm.mrad and so is close to the expected value. Twiss parameters (ax, ay, bx, by), emittance (Ex, Ey), and error (ksi) for both planes at IH Linac output are presented in table 19. Emittances are in mm.mrad, beta is in mm/mrad, and alpha has no dimension. The average is weighted with ksi.

		horizontal				vertical			
		Ex	ax	bx	ksi	Ey	ay	by	ksi
ITF.QFN03S	Trace	7.8871	-1.163	1.2174	0.355066	4.10865	-0.7635	2.40205	0.271123
	Mathematica	5.9579	-0.77854	1.18143	0.023887	3.354246	-0.3645	2.438861	0.03789
ITF.QDN02	Trace	Not convergent							
	Mathematica	10.3081	-5.38218	3.19667	0.189752	1.6993	-0.51715	0.541342	0.056576
Average	Trace	7.8871	-1.163	1.2174	0.355066	4.10865	-0.22216	2.40205	0.271123
	Mathematica	6.444295	-1.29327	1.406753	0.042432	2.690456	-0.42572	1.677776	0.045385
Expected from Dynac		8.5	-3.4	4.75		8.4	-2.28	4.13	

Table 19: *Twiss parameters and emittance at IH Linac output*

The first thing we can say is that it fit well with simulation for the horizontal plane, but the results in vertical plan are not really what we are expecting. The fact that the vertical plane doesn't fit with simulation since the LEBT (because it hits the vacuum chamber, se §2.4 and appendix), can be the reason why we don't get something fitting exactly simulation.
We can also observe, from the measured values of Twiss parameters, that at the exit of IH Linac, beam is divergent. This comes from the fact the third tank of IH Linac doesn't contain any transverse focusing devices.

CONCLUSIONS

In conclusion of this measurement campaign, several points can be highlighted. First thing, one can remark that the results of these measurements are quite coherent with the results that we were expecting from simulations. On the other hand, we have noticed an increase of emittance in RFQ, which indicates that the nominal settings in LEBT seams not to match the beam exactly to RFQ acceptance or that the beam is asymmetric when it enters the last solenoid of LEBT. Another important point is the recalibration of the second solenoid that corresponds to the recalibration of first solenoid. All the measurements of intensity and transmission are presented in the last appendix.

From those points, we can say that we are able to predict, with good approximations, the general behaviour of the transfer lines.

For future work, we are now able to describe the beam dynamics in the LINAC 3 (see figure 20) from the spectrometer. The uncertainty before spectrometer may be clarified by a more accurate measurement of emittance at the source output with an emittance measurement device, which will occur in 2004.

REFERENCES

[1] N. Angert (GSI), M.P. Bourgarel (GANIL), E. Brouzet, H. Haseroth, C.E. Hill, G. Hutter (GSI), J. Knott, H. Kugler, A. Lombardi (INFN, Legnaro), H. Lustig, E. Malwitz (GSI), F. Nitsch, G. Parisi (INFN, Legnaro), A. Pisent (INFN, Legnaro), U, Raich, U. Ratzinger (GSI), L. Riccati (INFN, Torino), A. Schempp (IAP, Frankfurt), K. Schindl, H. Schonauer, P. Tetu, H.H. Umstatter, M. van Rooij, D. Warner, M. Weiss, "*CERN Heavy Ion Facility Design Report*", CERN 93-01, Apr. 1993.

[2] K.R. Crandall, D.P. Rusthoi, "*TRACE 3-D Documentation*", LA-UR-97-886, May 1997.

[3] "*Mathematica Optimisation and Statistic*" http://www.wolfram.com/products/mathematica/newin42/nminimize.html

[4] P. R. Bevington, D. K. Robinson, "*Data reduction and error analysis for the physical sciences*", Second edition.p.68.

[5] J. Chamings "*Beam Profile Measurements to calculate Emittance in the LEBT of Linac 3*". not published

[6] J. Chamings "*Charge State Distribution Scan on LEBT of Linac3*", not published.

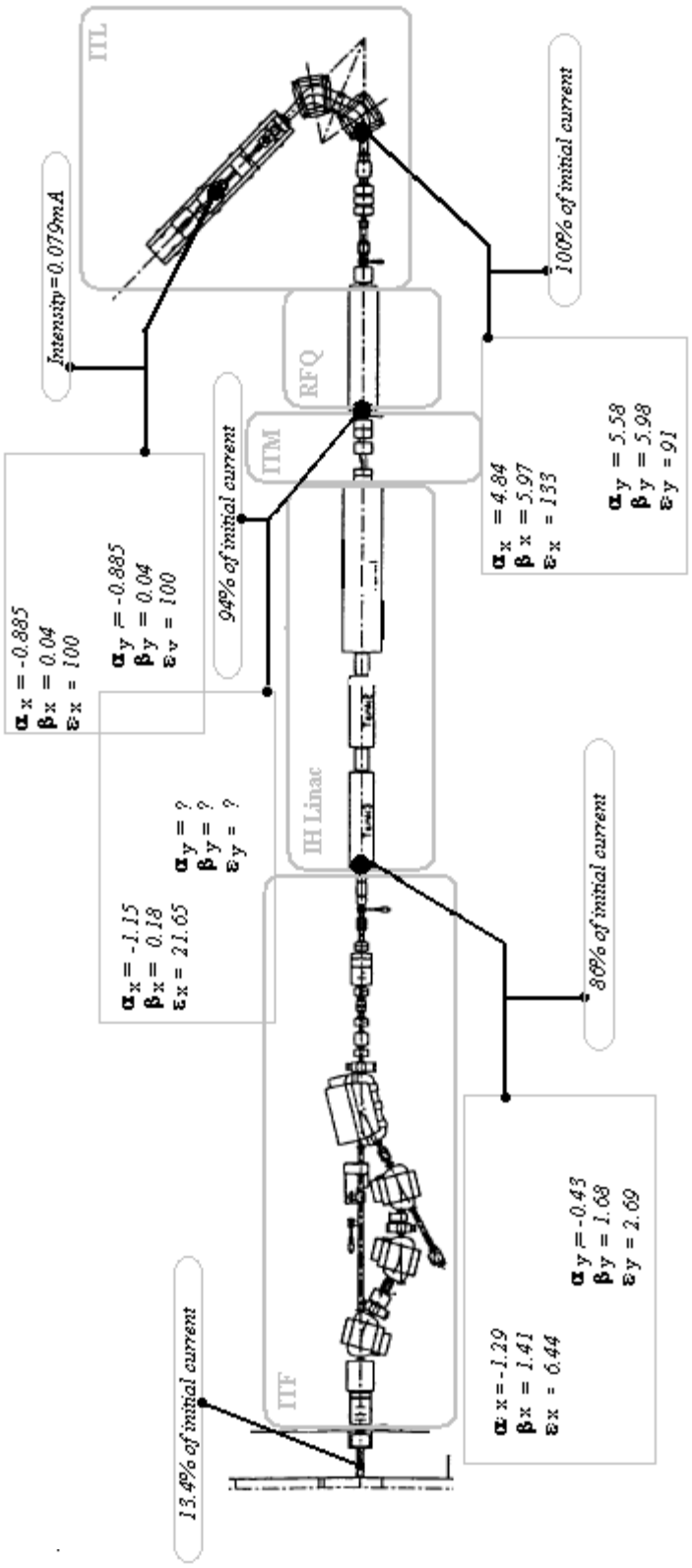

Figure 20: *Measured Twiss Parameters and Emittance in Linac 3*
(Emittance (ε) are in mm.mrad, β in mm/mrad, α has no dimension)

APPENDIX

STUDY OF THE BEHAVIOUR OF THE BEAM IN THE TRIPLET OF QUADRUPOLE OF LEBT

By introducing in TRACE the experimental parameters of first setting with the measured Twiss parameters of the source and considering the emittance in y equal to x emittance at the spectrometer output (TRACE doesn't give an eventual emittance increase in spectrometer), one get:

```
&data
 er= 193752.00 , q= 27., w= .544050, xi=0.000    ,
 emiti(1)=    125.00,    125.00, dpop= 0.0000,
 beami(1)=   -0.890,   0.0400,   -0.89000,   0.0400,
 beamf(1)= 0.0 , 0.179
 freq=   350.000, pqext=  2.50, ichrom= 0,
n1= 1, n2= 15, smax=  5.0, pqsmax=   2.5,
 nt( 1)=  1, a(1, 1)= 445.0
 nt( 2)=  5, a(1, 2)= 3794.4, 234.
 nt( 3)=  1, a(1, 3)= 851.0
 nt( 4 )= 1, a(1,4 )= 414.0
 nt( 5 )= 3,a(1, 5 )=  -0.3121,208.
 nt( 6 )= 1,a(1, 6 )= 578.00
 nt( 7 )= 9,a(1, 7 )=  25.,400.,90.,0.4722,4.4
 nt( 8 )= 8,a(1, 8 )= 67.5 ,400.
 nt( 9 )= 9,a(1, 9 )=  25.,400.,90.,0.4722,4.4
 nt( 10)= 1,a(1, 10)= 235.0
 nt( 11)= 3,a(1, 11)= 0.0,230.
 nt( 12)= 1,a(1, 12)= 235.0
 nt( 13)= 9,a(1, 13)=  25.,400.,90.,0.4722,4.4
 nt( 14 )= 8,a(1, 14)= 67.5,400.
 nt( 15)= 9,a(1, 15)=  25.,400.,90.,0.4722,4.4
 nt( 16 )= 1,a(1, 16 )= 888.
 nt( 17 )= 1,a(1, 17 )=  315.
 nt(18)=  3, a(1,18)= 0.9224    , 198.0    ,0.0000    ,0.0000    ,0.0000
 nt( 19)=  1, a(1,19)= 27.00
 nt( 20)=  3, a(1,20)=-1.443    , 98.0    ,0.0000    ,0.0000    ,0.0000
 nt( 21)=  3, a(1,21)=-1.443    , 98.0    ,0.0000    ,0.0000    ,0.0000
  nt(22)=  1, a(1,22)= 27.00
 nt(23)=  3, a(1,23)=0.764    , 198.0    ,0.0000    ,0.0000    ,0.0000
 nt(24)=  1, a(1,24)= 697.0
 nt(25)=  1, a(1,25)= 429.0
 nt(26)=  5, a(1,26)= 4192.    , 234.0    ,0.0000    ,0.0000    ,0.0000
 nt(27)=  1, a(1,27)= 193.0
 &end
```

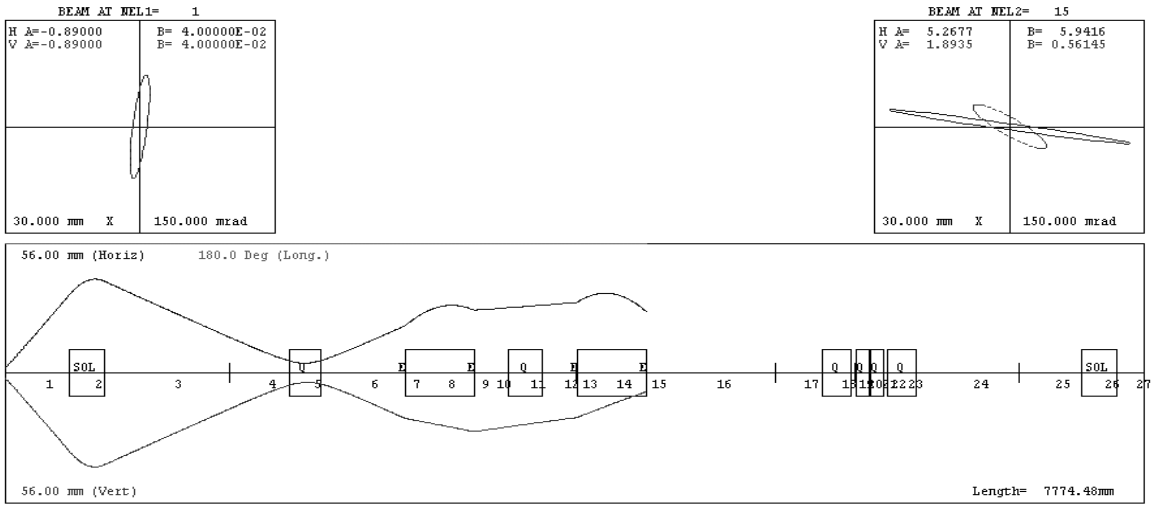

Figure A1

We get at the spectrometer output the configuration of figure A1. This result is in agreement with what we get with Path Manager and for the horizontal plane, it is in agreement with the measurements (see table 6). But in vertical plane the results doesn't seams to match with the measurements. To investigate the reason of this difference lets go few steps further, to the middle of the second quadrupole of the triplet. We get figure A2.

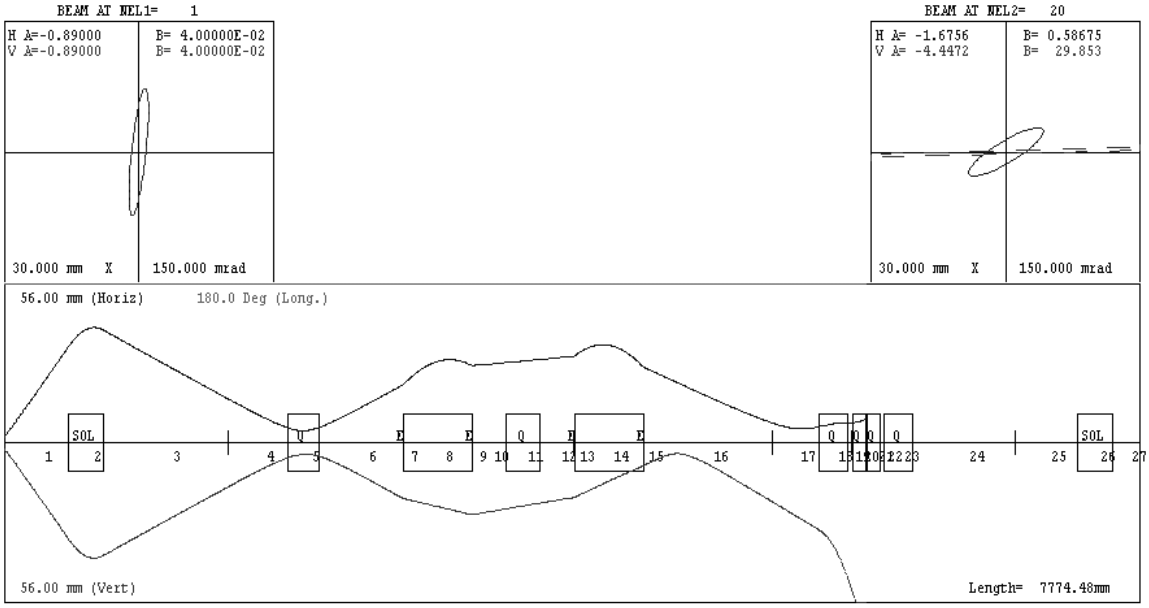

Figure A2

As we have $y_m = \sqrt{\varepsilon_y \beta_y}$ we can deduce that at this point of the line, the maximal extend of the beam in the vertical plane is 61.2 mm. As at this point the vacuum chamber has a radius of 56mm, the beam going downstream will have an emittance of $125*(5/6)^2$ which is approximately 90mm.mrad. By reintroducing those data in TRACE, one get figure A3.

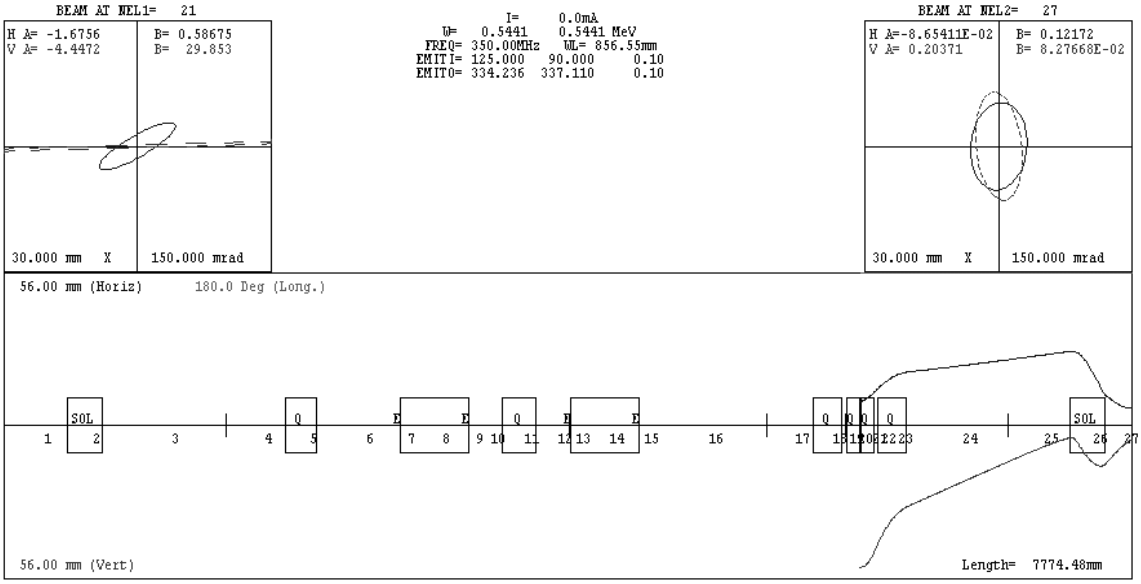

Figure A3

Emittance increases because the beam at solenoid input is not symmetric. The output beam is more or less matched and symmetric. The RFQ acceptance is α=0.864, β=0.028mm/mrad and ε=200mm.mrad. But the fact that emittance is so high can be the source of a higher emittance than expected in MEBT.

CURRENT AND TRANSMISSION ALONG LINAC 3

Faraday cup beam current measurements are available after the source (ITL.MFC01) after the ITL spectrometer (ITL.MFC02), in the ITM line (ITM.MFC01 or "MFC03"). There are then three current transformers, ITL.TRA05, ITF.TRA25 in the straight line after the stripper, and ITF.TRA25 after the third filter bending magnet to measure single charge-states.

	Current Measured μA	Transmission from ITL.MFC02
ITL.MFC01	~	~
ITL.MFC02	80	100%
ITM.MFC01	75	94%
ITF.MFC04	~	~
ITF.MFC05	69	86%
ITF.TRA25	21	13.4%

Table 0. *Transmission along Linac 3. All measurements rescaled to 75μA in ITL.MFC02*

The data was not gathered in a consistent run, due to difficulties with each measurement. Hence various different measurements have all been rescaled for 75μA at ITM.MFC01.
The results (see Table 0) suggest that the transmission of the Linac is rather good and that losses are spread along the machine.
This does not allow much scope for improving the beam current by tuning. However, the new cup ITF.MFC05 could be used for tuning the tanks, which was not the case with ITF.TRA15 (which may have some un-accelerated beam) or ITF.TRA25 (which has a weak and noisy signal).

It was also observed that a beam of Pb28+ also exists, and has an intensity of ~1.5% of the Pb27+. A corresponding beam of Pb26+/O2+ is only 0.1% as intense as the Pb27+ beam. It is assumed that this is due to gas stripping, and may have been enhanced by the recent vacuum intervention to install the cups in the ITF line.

The current measured in ITF.MFC04 was significantly higher than that measured up-stream. A full outer screening electrode has been added, which did not greatly change the situation. It is proposed to continue trying to understand this problem with a thicker suppression electrode and a positive suppression electrode up-stream.